

Simple dynamic exchange-correlation kernel of a uniform electron gas

Lucian A. Constantin¹ and J. M. Pitarke^{2,3}

¹Donostia International Physics Center (DIPC), Manuel de Lardizabal Pasealekua, E-20018 Donostia, Basque Country

²CIC nanoGUNE Consolider, Mikeletegi Pasealekua 56, E-2009 Donostia, Basque Country

³Materia Kondentsatuaren Fisika Saila, UPV/EHU and Unidad Física Materiales, CSIC-UPV/EHU, 644 Posta kutxatila, E-48080 Bilbo, Basque Country

(Received 24 February 2007; revised manuscript received 15 April 2007; published 29 June 2007)

We propose a simple dynamic exchange-correlation kernel of the uniform electron gas. We model the reduction of the electron-electron interaction due to the short-range exchange-correlation effects by introducing a frequency-dependent error-function effective interaction. By imposing the fulfillment of the compressibility and the third-frequency-moment sum rules, as well as the correct asymptotic behavior at large wave vectors, we find an accurate and simple dynamic exchange-correlation kernel that accurately reproduces the wave-vector analysis and the imaginary-frequency analysis of the correlation energy of the uniform electron gas.

DOI: [10.1103/PhysRevB.75.245127](https://doi.org/10.1103/PhysRevB.75.245127)

PACS number(s): 71.10.Ca, 71.15.Mb, 71.45.Gm, 31.15.Ew

Knowledge of the properties of the uniform electron gas has become essential for the understanding of electron correlations in condensed matter. In particular, the uniform electron gas has played a key role in the construction of most practical density-functional and time-dependent density-functional schemes,^{1–3} which are concerned with the approximation of the so-called Kohn-Sham exchange-correlation (xc) potential $v_{xc}(\mathbf{r})$ and the dynamic xc kernel $f_{xc}(\mathbf{r}, \mathbf{r}'; \omega)$, i.e., the functional derivative of the frequency-dependent xc potential $v_{xc}(\mathbf{r}, \omega)$ of time-dependent density-functional theory (TDDFT).

TDDFT shows that $f_{xc}(\mathbf{r}, \mathbf{r}'; \omega)$ is related to the dynamic density-response function $\chi(\mathbf{r}, \mathbf{r}'; \omega)$ of an arbitrary many-electron system via a Dyson-type screening equation of the form (unless otherwise stated, a.u. are used throughout, i.e., $e^2 = \hbar = m_e = 1$),⁴

$$\chi(\mathbf{r}, \mathbf{r}'; \omega) = \chi^0(\mathbf{r}, \mathbf{r}'; \omega) + \int d\mathbf{r}_1 d\mathbf{r}_2 \chi^0(\mathbf{r}, \mathbf{r}_1; \omega) \times v_{eff}[n](\mathbf{r}_1, \mathbf{r}_2; \omega) \chi(\mathbf{r}_2, \mathbf{r}'; \omega), \quad (1)$$

where $\chi^0(\mathbf{r}, \mathbf{r}'; \omega)$ is the density-response function of noninteracting Kohn-Sham electrons, and

$$v_{eff}[n](\mathbf{r}, \mathbf{r}'; \omega) = \frac{1}{|\mathbf{r} - \mathbf{r}'|} + f_{xc}[n](\mathbf{r}, \mathbf{r}'; \omega). \quad (2)$$

If $f_{xc}[n](\mathbf{r}, \mathbf{r}'; \omega)$ is taken to be zero, then Eq. (1) reduces to the well-known screening equation that is obtained in the framework of a time-dependent Hartree or random-phase approximation (RPA).^{5–7} The xc kernel $f_{xc}[n](\mathbf{r}, \mathbf{r}'; \omega)$ accounts, therefore, for the presence of short-ranged correlations that are absent in the RPA. Hence, it seems plausible to expect that the *effective* interaction $v_{eff}[n](\mathbf{r}, \mathbf{r}'; \omega)$ entering Eq. (1) might be replaced by a long-range interaction which in the case of a *uniform electron gas* of density n would take the approximate form

$$v_{eff}[n](\mathbf{r}, \mathbf{r}'; \omega) = \frac{\text{erf}(|\mathbf{r} - \mathbf{r}'|/\sqrt{4k_{n,\omega}})}{|\mathbf{r} - \mathbf{r}'|}, \quad (3)$$

where $\text{erf}(x)$ denotes the error function⁸ and $k_{n,\omega}$ represents a frequency-dependent density functional that accounts for the presence of short-range xc effects. For $k=0$, the long-range effective interaction of Eq. (3) reduces to the bare Coulomb interaction $1/|\mathbf{r} - \mathbf{r}'|$; for $k \rightarrow \infty$, the error-function effective interaction simply vanishes. This function is often used for the splitting of the Coulomb interaction, because it gives analytic matrix elements for both Gaussian and plane waves.^{9–11}

In this paper, we start with the frequency-dependent error-function effective interaction of Eq. (3) and impose the fulfillment of the compressibility and the third-frequency-moment sum rules to determine the coefficient $k_{n,\omega}$ and a simple form for the Fourier transform $f_{xc}(n; q, \omega)$ of the dynamic xc kernel of the uniform electron gas. We find that our xc kernel accurately reproduces the wave-vector analysis and the imaginary-frequency analysis of the correlation energy of the uniform electron gas.

First of all, we Fourier transform Eqs. (2) and (3) to find

$$f_{xc}(n; q, \omega) = \frac{4\pi}{q^2} [e^{-k_{n,\omega} q^2} - 1]. \quad (4)$$

On the one hand, the compressibility sum rule¹² requires that the long-wavelength ($q \rightarrow 0$) limit of the static ($\omega=0$) xc kernel $f_{xc}(n; q, \omega)$ takes the following form:¹³

$$f_{xc}(n; q \rightarrow 0, \omega = 0) = \frac{d^2}{dn^2} [n \epsilon_{xc}(n)], \quad (5)$$

where $\epsilon_{xc}(n)$ being the xc energy per particle of the uniform electron gas. We parametrize this static long-wavelength limit as follows:

$$f_{xc}(n; q \rightarrow 0, \omega = 0) = 4\pi \alpha n^\beta, \quad (6)$$

with $\alpha = -0.025\,518\,491\,6$ and $\beta = -0.691\,590\,707$.

On the other hand, according to the third-frequency-moment sum rule,¹⁴ the long-wavelength ($q \rightarrow 0$) limit of the xc kernel $f_{xc}(n; q, \omega)$ at $\omega \rightarrow \infty$ takes the form

$$f_{xc}(n; q \rightarrow 0, \omega \rightarrow \infty) = - (4/5)n^{2/3} \frac{d}{dn} \left[\frac{\epsilon_{xc}}{n^{2/3}} \right] + 6n^{1/3} \frac{d}{dn} \left[\frac{\epsilon_{xc}}{n^{1/3}} \right], \quad (7)$$

which we parametrize in the following way:

$$f_{xc}(n; q \rightarrow 0, \omega \rightarrow \infty) = \gamma_1 n^{\gamma_2}, \quad (8)$$

with $\gamma_1 = -0.114\,548\,231$ and $\gamma_2 = -0.614\,523\,371$.

Finally, combining Eqs. (4), (5), and (7), leads us to propose a xc kernel $f_{xc}(n; q, \omega)$ of the form of Eq. (4) with a coefficient $k_{n,\omega}$ that for imaginary frequencies ($\omega = iu$) is of the form

$$k_{n,iu} = - \frac{f_{xc}(n; q \rightarrow 0, \omega = 0)}{4\pi} \frac{1 + a(n)u + c(n)u^2}{1 + u^2}, \quad (9)$$

with

$$c(n) = \frac{f_{xc}(n; q \rightarrow 0, \omega \rightarrow \infty)}{f_{xc}(n; q \rightarrow 0, \omega = 0)}. \quad (10)$$

We have used the so-called adiabatic-connection fluctuation-dissipation theorem⁵⁻⁷ (ACFDT) to compute the correlation energy $\epsilon_c(n)$ per particle of the uniform electron gas from the xc kernel of Eq. (4) with the coefficient $k_{n,iu}$ of Eq. (9) and for various values of the electron density. We have then fitted the results obtained in this way to the Perdew-Wang parametrization of $\epsilon_c(n)$,¹⁵ which has led us to choose the following energy-optimized form for the coefficient $a(n)$ entering Eq. (9):

$$a(n) = 6\sqrt{c(n)}. \quad (11)$$

For imaginary frequencies, the xc kernel $f_{xc}(n; q, \omega)$ is real. Because our proposed kernel is an analytic function of ω , the complex $f_{xc}(n; q, \omega)$ at real frequencies can be obtained from Eqs. (4)–(11) by using the Kramers-Kronig relations.¹⁶

The xc kernel $f_{xc}(n; q, \omega)$ [or, equivalently, the so-called local-field factor $G(n; q, \omega) = -(q^2/4\pi)f_{xc}(n; q, \omega)$] of the uniform electron gas has been investigated by many authors, since the early *static* local-field factor introduced by Hubbard¹⁷ by summing all the exchange ladder diagrams entering the evaluation of the density-response function. Nowadays, diffusion Monte Carlo (DMC) calculations of the local-field factor of the uniform electron gas are available,^{18,19} which have been parametrized by Corradini *et al.*²⁰ Calculations of the frequency dependence of the local-field factor were carried out by Brosens and co-workers,^{21,22} and, more recently, by Richardson and Ashcroft.²³

Figure 1 compares the static form of our xc kernel $f_{xc}(n; q, \omega)$, which we have obtained from Eq. (4) with $\omega = 0$, to the parametrization of Ref. 20 and the static ($\omega = 0$) form of the xc kernel reported by Richardson and Ashcroft (RA).²³ Our ansatz [Eq. (4)] could not possibly reproduce the right behavior at $q \rightarrow \infty$;²⁵ however, our parametrization is smooth, which represents an important feature for a good approximation²⁶ and is at variance with the parametrizations reported in Refs. 20 and 23. Indeed, there is

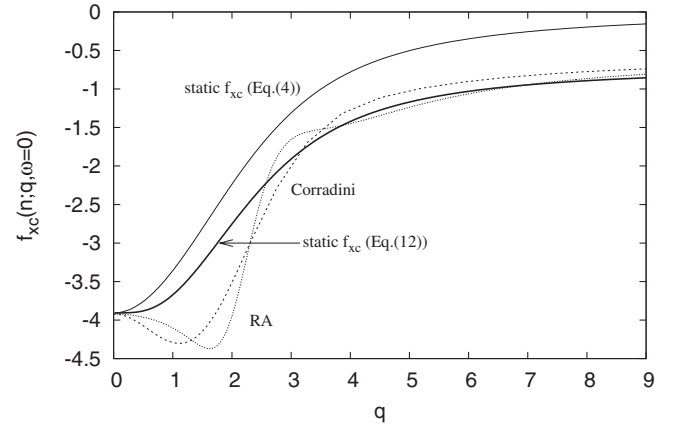


FIG. 1. Static xc kernel $f_{xc}(n; q, 0)$ versus q , for an electron density n equal to that of valence electrons in aluminum ($r_s = 2.07$) (Ref. 24), as obtained from Eqs. (4) (thin solid line) and (12) (thick solid line) with $\omega = 0$. Also shown are the parametrization of Ref. 20 (dashed line) and the static ($\omega = 0$) form of the xc kernel of Ref. 23 (dashed-dotted line).

no reason to believe that the static xc kernel $f_{xc}(n; q, 0)$ should not be monotonic: (i) the existence of a singularity at $q = 2k_F$ is not certain even for the uniform electron gas, as noted in Ref. 20, and (ii) no hump was detected in the DMC data.^{18,19}

A generalization of our kernel [Eq. (4)], which does reproduce the right behavior at $\omega = 0$ and $q \rightarrow \infty$ [see Eq. (A1) of Appendix] and preserves all good features of Eq. (4), is the following:²⁸

$$f_{xc}(n; q, \omega) = \frac{4\pi}{q^2} B(n) [e^{-k_{n,\omega} q^2} - 1] - \frac{4\pi}{k_F^2} \frac{C(n)}{1 + 1/q^2}, \quad (12)$$

where the frequency-dependent density functional $k_{n,\omega}$ is now given by Eq. (A3) of Appendix. The static form of our generalized xc kernel of Eq. (12) is represented in Fig. 1 by a thick solid line.

The long-wavelength ($q \rightarrow 0$) limit of our generalized xc kernel $f_{xc}(n; q, iu)$, which we have obtained from Eq. (12) at $q \rightarrow 0$, is represented in Fig. 2 as a function of the electron-density parameter r_s for various values of the imaginary frequency iu . This figure shows that the frequency dependence of our long-wavelength xc kernel $f_{xc}(n; 0, iu)$ is nonmonotonic; indeed, our xc kernel is found to be minimum at

$$u = [\sqrt{[1 - c(n)]^2 + a(n)^2} - (1 - c(n))]/a(n), \quad (13)$$

which seems to be physical.^{16,29} Moreover, our xc kernel $f_{xc}(n; 0, iu)$ exhibits a behavior that is qualitatively similar to that shown in Fig. 3 of Ref. 29.

At this point, we note that the parametrization of Gross and Kohn³ satisfies the important constraint

$$\text{Im} f_{xc}(n; q \rightarrow 0, \omega \rightarrow \infty) = -23\pi/(15\omega^{2/3}), \quad (14)$$

but the real part of the Gross-Kohn parametrization exhibits a frequency dependence that is considerably different from the expected highly nonmonotonic behavior.²⁹ We recall that Eq. (14) is true for any $q < \infty$, so it can represent a powerful

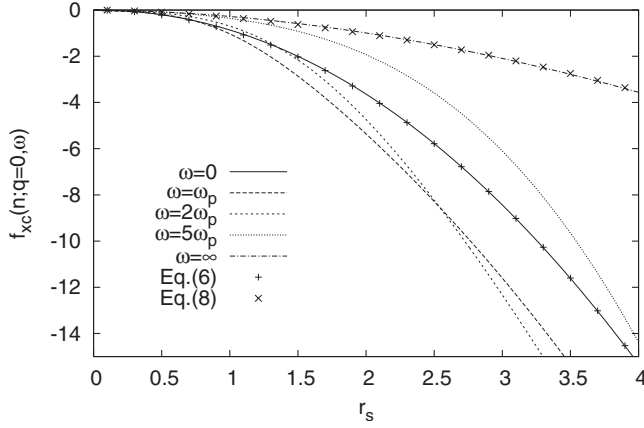


FIG. 2. Long-wavelength xc kernel $f_{xc}(n; 0, \omega)$ versus r_s , as obtained from Eq. (12) with $q \rightarrow 0$ (solid lines) for various values of the imaginary frequency $i\omega$. Here, $\omega_p = \sqrt{4\pi n}$ represents the plasma frequency. Crosses and stars represent the results obtained from Eqs. (6) and (8), respectively. Equation (4) yields a long-wavelength xc kernel $f_{xc}(n; 0, \omega)$ that is qualitatively similar to the more accurate form represented in this figure.

tool in the construction of accurate complex xc kernels, although the Kramers-Kronig relations will probably deteriorate the simplicity of the real part of the xc kernel (e.g., the real part of the Gross-Kohn xc parametrization is found to be given in terms of elliptic integrals¹⁶).

In order to test our xc kernel, we follow Lein *et al.*³⁰ to analyze the ACFDT correlation energy per particle $\epsilon_c(n)$ of a uniform electron gas into contributions $\epsilon_c(n; q)$ and $\epsilon_c(n; u)$ from density fluctuations of different wave vectors \mathbf{q} and imaginary frequencies $i\omega$, respectively.

In Figs. 3–5, we represent the wave-vector analysis $\epsilon_c(n; q)$ that we have obtained by using the dynamic xc kernel of Eq. (12) (dashed line) and the static xc kernel of Eq. (12) with $\omega=0$ (dashed-dotted line). We compare these cal-

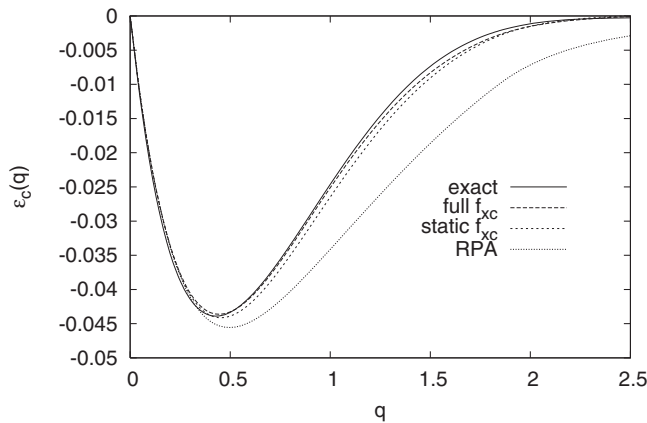


FIG. 3. Wave-vector analysis of the correlation energy per electron of the uniform electron gas at $r_s = 2.07$, as obtained from Eq. (12). The “exact” wave-vector analysis is obtained from the Perdew-Wang parametrization of the xc hole (Ref. 31). Also shown are the results we have obtained from our static xc kernel $f_{xc}(n; q, 0)$ of Eq. (12) with $\omega=0$.

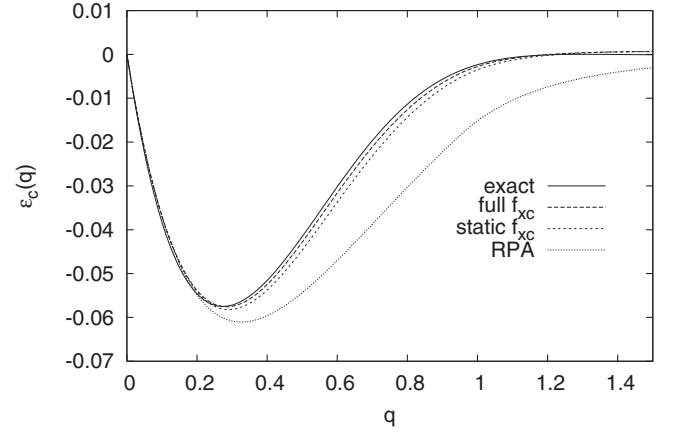


FIG. 4. As in Fig. 3, but for $r_s = 4$.

culations to the wave-vector analysis obtained (i) in the RPA (dotted line), as in Ref. 30, and (ii) from the Fourier transform of the Perdew-Wang parametrization of the exact coupling-constant averaged correlation-hole density (solid line).³¹ While the RPA curve is too negative for intermediate- and high- q values, as pointed out in Ref. 30, the curve that we have obtained from our dynamic xc kernel is very close to the exact wave-vector analysis. We have also carried out calculations from our simpler dynamic xc kernel of Eq. (4), and we have found that they are nearly indistinguishable from the corresponding calculations obtained from Eq. (12) and displayed in Figs. 3–5.

The imaginary-frequency analysis $\epsilon_c(n; u)$ of the correlation energy of a uniform electron gas is not known exactly. Hence, as in Ref. 30, we use as an étalon the frequency analysis derived from the use of the RA dynamic xc kernel,²³ which satisfies many known exact constraints. In Figs. 6 and 7, we represent the frequency analysis that we have obtained by using the dynamic xc kernel of Eq. (12) (dashed line), the static xc kernel of Eq. (12) with $\omega=0$ (dashed-dotted line), and the RA dynamic xc kernel (solid line). We note that the frequency analysis obtained from our dynamic xc kernel and from the RA dynamic xc kernel nearly coincides both in the low-frequency regime (see Fig. 6) and in the high-frequency regime (see Fig. 7), which suggests that our proposed xc

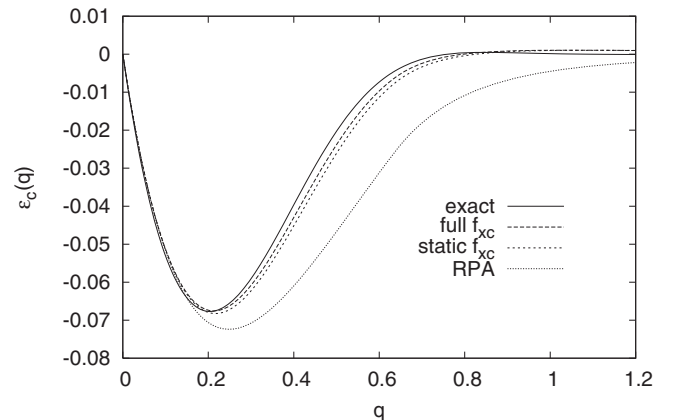


FIG. 5. As in Fig. 3, but for $r_s = 6$.

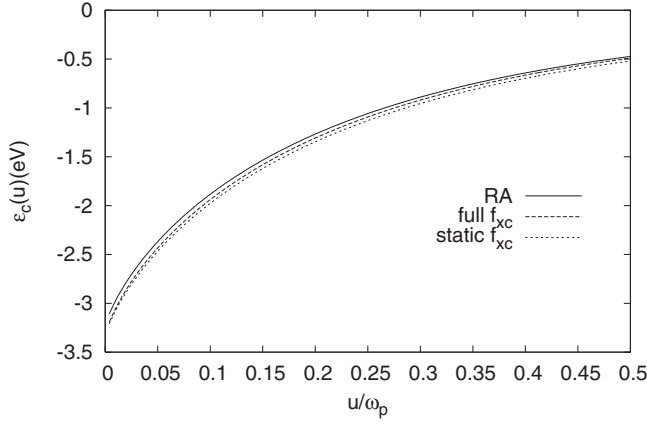


FIG. 6. Imaginary-frequency analysis (low- u regime) of the correlation energy per electron of the uniform electron gas at $r_s=4$. The RA imaginary-frequency analysis is obtained from the Richardson-Ashcroft parametrization (Ref. 20), as in Ref. 30. Also shown is the result we have obtained from our static xc kernel $f_{xc}(n; q, 0)$.

kernel has a successful frequency parametrization. As occurs with $\varepsilon_c(n; q)$, we have found that the simpler xc kernel of Eq. (4) yields an imaginary-frequency analysis that is nearly indistinguishable from the corresponding analysis obtained from Eq. (12) and displayed in Figs. 6 and 7.

Finally, we have calculated the total ACFDT correlation energy per particle $\varepsilon_c(n)$ of the uniform electron gas [as obtained from our proposed static and dynamic xc kernel and also from the Corradini²⁰ and RA (Ref. 23) parametrizations] and we have subtracted the Perdew-Wang parametrization $\varepsilon_c^{\text{exact}}(n)$.¹⁵ Figure 8 shows the results that we have obtained for $r_s=0-15$. Apart from the very high-density regime ($r_s \rightarrow 0$), our dynamic xc kernel of Eq. (12) yields a good estimate of the exact xc energy, which is considerably better than the Corradini approximation although not as good as the RA approach. As noted above, the simpler xc kernel of Eq. (4) yields both wave-vector and imaginary-frequency analyses that are close to the corresponding analysis obtained from the xc kernel of Eq. (12); nonetheless, Fig. 8 clearly shows that the more accurate parametrization of Eq. (12) significantly improves the accuracy of the xc energy of the uniform electron gas.

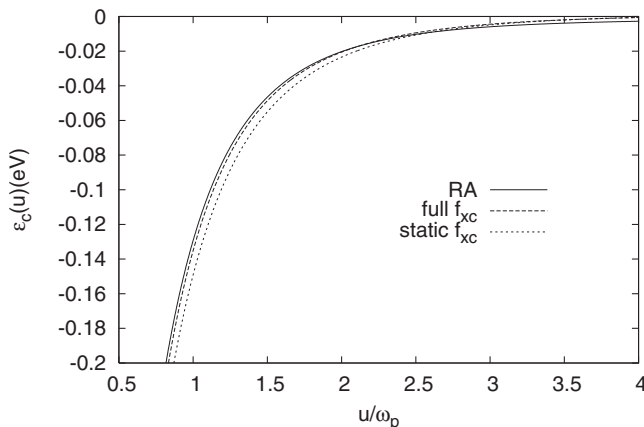


FIG. 7. As in Fig. 6, but for the high- u regime

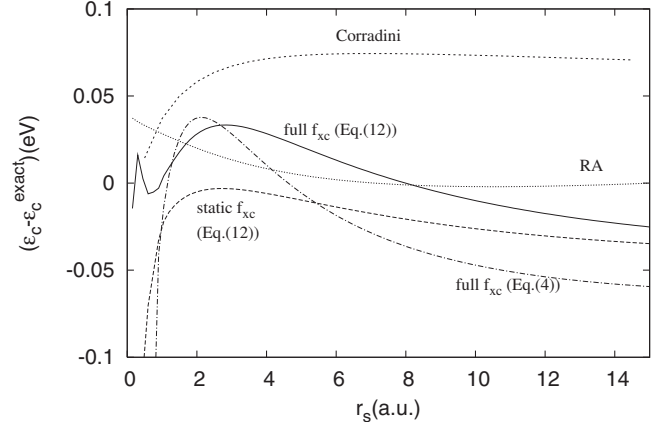


FIG. 8. Deviation of our ACFDT correlation energy per particle $\varepsilon_c(n)$ with respect to the Perdew-Wang parametrization $\varepsilon_c(n)^{\text{exact}}$ (Ref. 15) versus r_s . Also shown are the ACFDT results we have obtained from the Corradini and Richardson-Ashcroft parametrizations of Refs. 20 and 23, respectively.

In summary, we have modeled the reduction of the electron-electron interaction due to the short-range xc effects by introducing a physically motivated frequency-dependent error-function effective interaction. By imposing the fulfillment of the compressibility and the third-frequency-moment sum rules, as well as the correct asymptotic behavior at large wave vectors, we have been able to construct a simple dynamic xc kernel of the uniform electron gas, which is Fourier transformable and accurately reproduces the wave-vector analysis and the imaginary-frequency analysis of the correlation energy of the uniform electron gas. We have shown that the error function can be used to construct a physically motivated frequency-dependent effective interaction and a simple and accurate dynamic xc kernel, which can easily be used for spherical systems.

We have presented the results for the unpolarized electron gas, but despite the fact that Eqs. (4) and (12) neglect spin-polarization effects, they describe satisfactorily the fully spin-polarized uniform electron gas (as occurs with the parametrization of Ref. 20). Thus, due to its simplicity and robustness, we expect that our dynamic xc kernel will accurately describe ionization³² and atomization³³ processes.

We acknowledge partial support by the University of the Basque Country, the Basque Unibertsitate eta Ikerketa Saila, the Spanish Ministerio de Educación y Ciencia, and the EC sixth framework Network of Excellence Nanoquanta (Grant No. NMP4-CT-2004-500198).

APPENDIX

An exact constraint,²⁵ which is violated by Eq. (4), is the following:

$$f_{xc}(n; q \rightarrow \infty, \omega = 0) \rightarrow -4\pi B(n)/q^2 - 4\pi C(n)/k_F^2, \quad (\text{A1})$$

where

$$C(n) = -\frac{\pi}{2k_F} \frac{d(r_s \epsilon_c)}{dr_s}, \quad (\text{A2})$$

and k_F represents the Fermi momentum of the uniform electron gas: $k_F = (3\pi^2 n)^{1/3}$. The density-dependent coefficient $B(n)$ was parametrized in Ref. 20 from the Monte Carlo calculations reported in Ref. 19.

A smooth xc kernel $f_{xc}(n; q, \omega)$, which generalizes our xc kernel of Eq. (4) and satisfies not only the compressibility and the third-frequency-moment sum rules [see Eqs. (5) and (7)] but also Eq. (A1), is that of Eq. (12), with

$$k_{n,iu} = -\frac{f_{xc}(n; q \rightarrow 0, \omega = 0)}{4\pi B(n)} \frac{1 + a(n)u + c(n)u^2}{1 + u^2}, \quad (\text{A3})$$

and $c(n)$ being still given by Eq. (10). We have fitted the ACFDT correlation energy $\epsilon_c(n)$ per particle of the uniform electron gas obtained from this kernel for various values of the electron density to the Perdew-Wang parametrization,¹⁵ which has led us to choose in this case the following energy-optimized form for the coefficient $a(n)$ entering Eq. (A3):

$$a(n) = \exp\left[\frac{10.5}{(1 + r_s)^{13/2}}\right] + \frac{1}{2}. \quad (\text{A4})$$

Introducing the Fourier transform of Eq. (12) into Eq. (2), one finds the following generalization of Eq. (3):

$$\begin{aligned} v_{eff}[n](\mathbf{r}, \mathbf{r}'; \omega) = & \frac{1 - B(n) + B(n)\text{erf}(|\mathbf{r} - \mathbf{r}'|/\sqrt{4k_{n,\omega}})}{|\mathbf{r} - \mathbf{r}'|} \\ & + \frac{C(n)}{k_F^2 |\mathbf{r} - \mathbf{r}'|} [\cosh(|\mathbf{r} - \mathbf{r}'|)\text{sign}(|\mathbf{r} - \mathbf{r}'|) \\ & - \sinh(|\mathbf{r} - \mathbf{r}'|)]. \end{aligned} \quad (\text{A5})$$

For $|\mathbf{r} - \mathbf{r}'| \neq 0$, the last term of Eq. (A5) is

$$\cosh(|\mathbf{r} - \mathbf{r}'|)\text{sign}(|\mathbf{r} - \mathbf{r}'|) - \sinh(|\mathbf{r} - \mathbf{r}'|) = e^{-|\mathbf{r} - \mathbf{r}'|}. \quad (\text{A6})$$

We note that if the density-dependent coefficients $B(n)$ and $C(n)$ are replaced by $B(n)=1$ and $C(n)=0$, then Eq. (A5) simply yields the original Eq. (3).

¹W. Kohn and L. J. Sham, Phys. Rev. **140**, A1133 (1965).

²E. Runge and E. K. U. Gross, Phys. Rev. Lett. **52**, 997 (1984).

³E. K. U. Gross and W. Kohn, Phys. Rev. Lett. **55**, 2850 (1985).

⁴E. K. U. Gross, J. F. Dobson, and M. Petersilka, in *Density Functional Theory II*, Topics in Current Chemistry Vol. 181, edited by R. F. Nalewajski (Springer, Berlin, 1996), p. 81.

⁵J. Harris and A. Griffin, Phys. Rev. B **11**, 3669 (1975).

⁶D. C. Langreth and J. P. Perdew, Phys. Rev. B **15**, 2884 (1977); **21**, 5469 (1980); **26**, 2810 (1982).

⁷O. Gunnarsson and B. I. Lundqvist, Phys. Rev. B **13**, 4274 (1976).

⁸*Handbook of Mathematical Functions*, edited by M. Abramowitz and I. Stegun (Dover, New York, 1972).

⁹J. Heyd, G. E. Scuseria, and M. Ernzerhof, J. Chem. Phys. **118**, 8207 (2003).

¹⁰J. Toulouse, F. Colonna, and A. Savin, Phys. Rev. A **70**, 062505 (2004).

¹¹P. Gori-Giorgi and A. Savin, Phys. Rev. A **73**, 032506 (2006).

¹²S. Ichimaru, Rev. Mod. Phys. **54**, 1017 (1982).

¹³Assuming that the electron density induced by external perturbations is slowly varying in space and time, the xc kernel $f_{xc}(n; q, \omega)$ is sometimes taken to be equal to the static ($\omega=0$) long-wavelength ($q \rightarrow 0$) limit for all values of q and ω . This is the so-called adiabatic local-density approximation (ALDA).

¹⁴N. Iwamoto and E. K. U. Gross, Phys. Rev. B **35**, 3003 (1987).

¹⁵J. P. Perdew and Y. Wang, Phys. Rev. B **45**, 13244 (1992).

¹⁶K. Burke and E. K. U. Gross, *A Guided Tour of Time-Dependent Density Functional Theory*, in Proceedings of the Merense Summer School on Density Functional Theory, edited by D. Joubert (Springer, New York, 1997).

¹⁷J. Hubbard, Proc. R. Soc. London, Ser. A **243**, 336 (1957).

¹⁸C. Bowen, G. Sugiyama, and B. J. Alder, Phys. Rev. B **50**, 14838 (1994).

¹⁹S. Moroni, D. M. Ceperley, and G. Senatore, Phys. Rev. Lett. **75**, 689 (1995).

²⁰M. Corradini, R. Del Sole, G. Onida, and M. Palumbo, Phys. Rev. B **57**, 14569 (1998).

²¹F. Brosens, L. F. Lemmens, and J. T. Devreese, Phys. Status Solidi B **74**, 45 (1976).

²²F. Brosens and J. T. Devreese, Phys. Rev. B **29**, 543 (1984).

²³C. F. Richardson and N. W. Ashcroft, Phys. Rev. B **50**, 8170 (1994).

²⁴The electron density n is usually characterized by the density parameter $r_s = (3/4\pi n)^{1/3}/a_0$, a_0 being the Bohr radius, $a_0 = 0.529 \text{ \AA}$.

²⁵G. Vignale, Phys. Rev. B **38**, 6445 (1988).

²⁶For instance, in the construction of the generalized gradient approximation (GGA) for the exchange hole the maximization of the information entropy was used (Ref. 27), which ensures that the GGA exchange hole is as smooth as possible.

²⁷M. Ernzerhof and J. P. Perdew, J. Chem. Phys. **109**, 3313 (1998).

²⁸The unphysical feature exhibited by the xc kernels of Eqs. (4) and (12) at $\omega=1$ is unimportant for the imaginary-frequency integration that leads to the correlation energy.

²⁹H. M. Bohm, S. Conti, and M. P. Tosi, J. Phys.: Condens. Matter **8**, 781 (1996).

³⁰M. Lein, E. K. U. Gross, and J. P. Perdew, Phys. Rev. B **61**, 13431 (2000).

³¹J. P. Perdew and Y. Wang, Phys. Rev. B **46**, 12947 (1992).

³²S. K. Semenov, N. A. Cherepkov, G. H. Fecher, and G. Schön-hense, Phys. Rev. A **61**, 032704 (2000).

³³F. Furche, Phys. Rev. B **64**, 195120 (2001).